

Reinvestigation of the reentrant spin-glass phase of $\text{Fe}_{26}\text{Cr}_{74}$ by high-resolution inelastic neutron scattering

S. Lequien, B. Hennion, and S. M. Shapiro*

*Laboratoire Léon Brillouin, Centre d'Etudes Nucléaires de Saclay,
91191 Gif-sur-Yvette, Cedex, France*

(Received 14 October 1987)

High-resolution inelastic neutron scattering measurements performed on the sample $\text{Fe}_{26}\text{Cr}_{74}$ used in the first experiment of Shapiro *et al.* [Phys. Rev. B **24**, 6661 (1981)] show that propagating spin waves are unambiguously present down to 13 K. Measurements at lower temperatures are again hampered by the experimental limitations, which do not allow a clear separation between elastic and inelastic signals. The most natural extrapolation of the data analysis favors, but does not prove, the existence of spin waves at the lowest temperatures, even when using the double Lorentzian representation of the spectral weight function.

I. INTRODUCTION

Reentrant spin-glasses (RSG) belong to a class of diluted ferromagnets which exhibit a spin-glass- (SG) like state at the lowest temperature, a paramagnetic (PM) state at the highest temperature and, in between, a state with ferromagnetic- (FM) like properties. A large number of different systems exhibit this behavior and there have been extensive experimental investigations using a variety of techniques. Despite all of this, the nature of the FM and SG states are not well understood. Neutron scattering is one of the important probes of magnetic correlations and inelastic studies have revealed some surprising anomalous behavior.¹⁻⁹ In all systems there is general agreement that on cooling into the FM state, spin-wave excitations start to appear and their energy increases with decreasing temperature. The spin-wave energy follows the dispersion relation expected for a ferromagnetic: $\hbar\omega = \Delta + Dq^2$, where Δ is a small energy gap and D is the magnetic stiffness. As the temperature is further reduced, D reaches a maximum and then starts to decrease. At the same temperature the linewidth of the excitation starts to increase, and the transverse part of the susceptibility, χ'_q , also increases. At a lower temperature a q -dependent elastic peak develops indicative of static correlations. This central peak continues to increase with decreasing temperature and dominates the spectra at lowest temperatures.

The behavior of the spin-wave stiffness at the lowest temperature is still unclear and controversial. In the first work on FeCr ,¹ no well-defined excitations were observed below $T=20$ K and the spectra were described by a single Lorentzian centered at $\omega=0$. Subsequent measurements⁹ on FeAl also showed a complete collapse of the spin waves and no propagating excitations at low temperatures. Measurements on the amorphous material, $a\text{-Fe}_{1-x}\text{Mn}_x$,² yielded no definitive conclusion since the interpretation was very dependent upon the data analysis. On the other hand, measurements on polycrystalline $\text{Ni}_{1-x}\text{Mn}_x$ unambiguously showed⁴ that on decreasing the temperature the magnetic stiffness goes through a

minimum and then increases again at lower temperatures. This result was confirmed on samples of NiMn from different origins and slightly different compositions, thus eliminating the possibility that the increase of D at low temperature was an artifact of sample inhomogeneity. Moreover, similar behavior was observed⁵ in $a\text{-Fe}_{1-x}\text{Mn}_x$ with $x=0.235$.

This apparent nonuniversality of the behavior of the magnetic stiffness with temperature in the various RSG's is a puzzling question. With the development of cold neutron moderators at high- and medium-flux reactors much better energy resolution can now be achieved. It is therefore worthwhile to reexamine the spin waves in $\text{Fe}_x\text{Cr}_{1-x}$, the first system studied.

II. EXPERIMENTAL

The identical polycrystalline sample of $\text{Fe}_{26}\text{Cr}_{74}$ used in Ref. 1 was used in the present experiment. Measurements were performed on the 4F1 three-axis spectrometer situated on a cold source at the Orphée Reactor at Saclay. The instrument was operated with a fixed k_I delivered by a double PG002 monochromator, the first one being bent to vertically focus the beam. A cooled Be filter was placed before the sample to eliminate higher-order contamination. The horizontal collimations were $25^\circ\text{-}50^\circ\text{-}60^\circ\text{-}20^\circ\text{-}20^\circ$. The elastic line shape was checked by measurements on a partially deuterated sample of polystyrene which exhibits an intense purely elastic scattering at small angles. The line shape was Gaussian with a very slight enhancement in the wings. The full width at half maximum (FWHM) was $28 \mu\text{eV}$ for $k_I=1.12 \text{ \AA}^{-1}$ and $20 \mu\text{eV}$ for $k_I=1.05 \text{ \AA}^{-1}$, which is about a factor of 3 better than used in the earlier measurements. The temperature-independent background was determined with no sample in the displacer refrigerator used to cool the sample. The background level was about 0.5 count/min. and constant over the range of spectrometer settings.

In the data analysis the experimentally measured line shape was used for the elastic scattering and the calculated Gaussian resolution function was used for the inelastic

part. The resolution was folded with an assumed form of the scattering cross section and calculated intensities were compared with the observed data by a least-squares adjustment of parameters in the cross section which can be written as

$$\frac{d^2\sigma}{d\Omega d\omega} = A \frac{k_F}{k_I} \left[TB_s \frac{F(Q, \omega)}{Q^2} + B_c(Q)\delta(\omega) \right]. \quad (1)$$

A contains the coupling constant of the neutrons with the spins; k_F , and k_I are the final and initial wave vectors of the neutrons. The first term in the large parentheses represents scattering from ferromagnetic spin waves in the limit $k_B T \gg \hbar\omega$, a condition always satisfied in the present experiment; B_s is proportional to the transverse part of the susceptibility and the $1/Q^2$ dependence is assumed as in classical ferromagnet, neglecting anisotropy. The second term is included to account for the elastic scattering. It is worthwhile to note that in this formalism the elastic and inelastic scattering are taken as independent, which could be a wrong assumption.

We are now left with the problem of the choice of the spectral weight function $F(Q, \omega)$ which accounts for the dynamics of the system. In the absence of an ascertained physical mechanism to describe the spin-wave damping, two phenomenological forms are generally used: the double Lorentzian (DL) and the damped harmonic oscillator (DHO)

$$F_{DL}(Q, \omega) = \frac{1}{2\pi} \left[\frac{\Gamma_Q}{(\omega - \omega_Q)^2 + \Gamma_Q^2} + \frac{\Gamma_Q}{(\omega + \omega_Q)^2 + \Gamma_Q^2} \right], \quad (2)$$

$$F_{DHO}(Q, \omega) = \frac{1}{\pi} \frac{\Gamma_Q \omega_Q^2}{(\omega^2 - \omega_Q^2)^2 + \omega^2 \Gamma_Q^2}. \quad (3)$$

In the case where $\omega_Q \gg \Gamma_Q$ both Eqs. (2) and (3) reduce to the same form, except Γ_Q in Eq. (3) now represents the FWHM of the observed spectrum.

However, when the damping increases, the differences between Eqs. (2) and (3) rapidly become important. For Eq. (2) the positions of the maximum are given by

$$\omega^2 + \omega_Q^2 + \Gamma_Q^2 - 2\omega_Q(\omega_Q^2 + \Gamma_Q^2)^{1/2} = 0.$$

This yields real solutions for $\Gamma_Q^2 \leq 3\omega_Q^2$ and the position of the maximum stays very near ω_Q as far as $\Gamma_Q \lesssim \omega_Q$. For Eq. (3) the positions of the maxima are given by

$$\omega^2 - \omega_Q^2 + \frac{1}{2}\Gamma_Q^2 = 0.$$

Real solutions will exist for $\Gamma_Q^2 \leq 2\omega_Q^2$ and the position of the maximum rapidly moves aside from ω_Q . In both cases when ω_Q exceeds the defined limit the maximum of $F(Q, \omega)$ occurs at $\omega=0$. Furthermore, in the limit $\Gamma_Q/\omega_Q \rightarrow \infty$, $F_{DHO}(Q, \omega)$ becomes a δ function.

Comparison between experimental line shapes and calculated ones does not allow us to favor one of the models. When the damping is small the models are equivalent. When the damping is increasing the main difference concerns the energy region between the two maxima: the valley is more filled in for the DHO compared to the DL.

Unfortunately in the case of the RSG under consideration here, an elastic component always develops when the damping increases, masking the zero-energy response of the spin-wave line shape. Therefore we have made a systematic use of both formulas throughout the whole data analysis.

III. RESULTS

Measurements have been performed at $T=80, 60, 40, 20$, and 13 K for Q values of $0.04, 0.055, 0.065$, and 0.075 \AA^{-1} . Down to 40 K they confirm the decrease of the spin-wave energies and the increase of their damping when lowering the temperature, as initially put forward by Shapiro *et al.*, but measurements at 20 and 13 K showed unambiguously that propagating spin waves are still present at these temperatures. This is illustrated on Fig. 1 where raw data are reported. The lines drawn through the points correspond to the results of least-squares fits using the DL model. Fits using the DHO

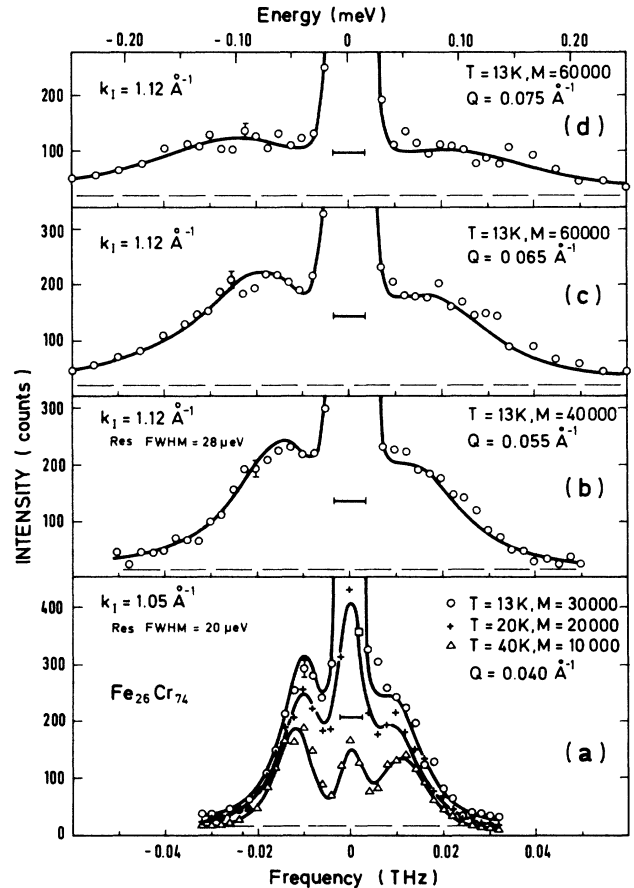


FIG. 1. Raw data spectra for $\text{Fe}_{26}\text{Cr}_{74}$: the intensities are the real ones, so that the error bars are given by their square roots. The lines are calculated lines resulting from fits using the DL model. (a) Evolution with temperature of the scattering at $q=0.040 \text{ \AA}^{-1}$; monitor values as such to match the thermal Bose factor. (b), (c), and (d) q dependence of the scattering at $T=13$ K adjusted parameters with F_{DL} are $\Delta=0.0042 \text{ THz}$, $D=2.82 \text{ THz \AA}^2$.

model yield quite similar results and we found no statistical significant difference between the chi-square values given by both analysis.

Figure 2 shows the values of the spin-wave line widths in the DL model as a function of q^2 . They correspond to the calculated curves of Fig. 1, or to the best $\omega = D_{\text{eff}} q^2$ ($D_{\text{eff}} = 4 \text{ THz } \text{\AA}^2$), when neglecting the gap. For the q range studied, the spin waves are underdamped, independent of the choice of $F(Q, \omega)$. It is obvious that the q range is too restricted to ensure any law for the q dependence of the damping. Straight lines corresponding to a quadratic and a quartic dispersion only indicate that, in the assumption of a power law $\Gamma = q^\alpha$, α should be between 2 and 4. This behavior could be a result of different contributions to Γ : dynamical effects might coexist with spatial effects due to the geometric disorder of the spins. This geometric contribution has received little theoretical consideration and its Q and T dependences are unknown.

Concerning the understanding of the RSG systems the existence of spin waves in the low-temperature phase is very important. These measurements now extend the existence of propagating spin waves from the 25 K limit described by Shapiro *et al.* down to 13 K.

A second set of measurements was performed, using a helium cryostat to investigate lower temperatures. Spectra at 5, 10, and 20 K were measured at $Q = 0.040 \text{ \AA}^{-1}$. Figure 3 shows the data collected at 5 K. The counting time was about 3800 s per point. The elastic component is now dominating the signal and the background becomes a significant portion of the wings. The existence of an inelastic signal is unambiguous but we are now unable to ascertain the existence or nonexistence of propagating spin waves at this temperature. Indeed as pointed out by the various lines indicated on the figure the inelastic part

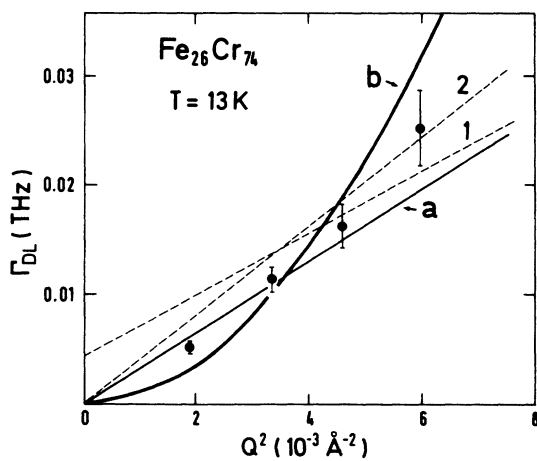


FIG. 2. Q dependence of the spin-wave linewidth at $T = 13 \text{ K}$ in the DL model (Q values are corrected from resolution effect as explained in Ref. 4). Dotted lines correspond to the spin-wave dispersion: (1) Best fit with $\omega = \Delta + Dq^2$, $\Delta = 0.0042 \text{ THz}$ and $D = 2.82 \text{ THz } \text{\AA}^2$. (2) Best fit with $\omega = D_{\text{eff}} q^2$, $D_{\text{eff}} = 4 \text{ THz } \text{\AA}^2$. Solid lines correspond to (a) $\Gamma = Cq^2$, with $C = 3.24 \text{ THz } \text{\AA}^2$; (b) $\Gamma = Cq^4$, with $C = 894 \text{ THz } \text{\AA}^4$.

of the spectrum can be fitted by either form of $F(Q, \omega)$ for spin waves or even by a totally quasielastic line [Eq. (2) with $\omega_Q = 0$].

The overall results are presented in Figs. 4–6. The evolution of the stiffness constant according to the two models, together with the results from Shapiro *et al.* for the DL model is shown in Fig. 4. The values of the stiffness constant are given by an analysis where all the data collected at a given temperature are fitted together using Eq. (1) with B_s , D , Γ_Q , and $B_c(Q)$ as adjustable parameters. The introduction of a small gap in the dispersion of the spin waves slightly improves the fits but the uncertainty on the gap values does not allow us to give a

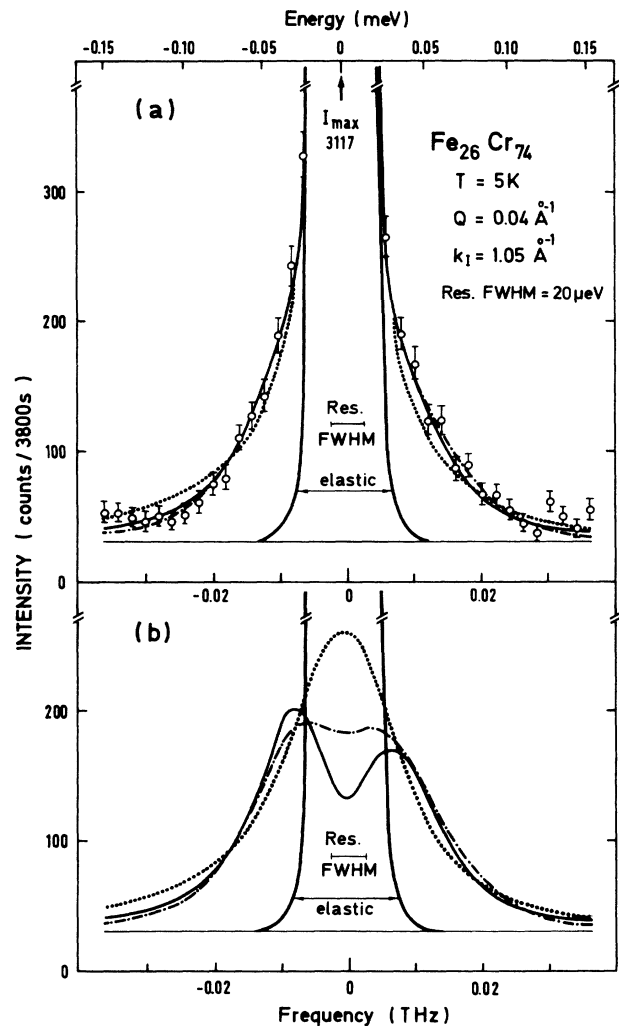


FIG. 3. (a) Spectrum at $T = 5 \text{ K}$ for $q = 0.04 \text{ \AA}^{-1}$. The horizontal solid line (—) corresponds to the estimated background. The pure elastic contribution (—) is shown with the total intensities calculated using the DHO (—), the DL (· · · · ·) and the forced quasielastic (— · — · —) analysis for the inelastic part. (b) Pure elastic (—) and inelastic (— · — · —, · · · · ·, · · · · ·) contributions corresponding, respectively, to the three calculated intensities of part (a): DHO, DL, and forced quasielastic analysis.

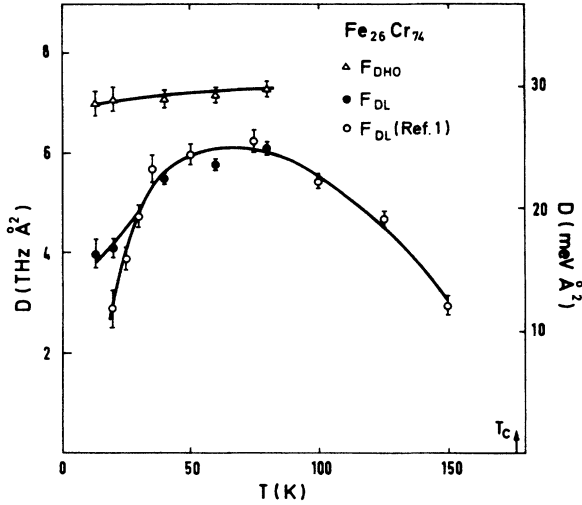


FIG. 4. Temperature dependence of the stiffness constant. \circ : from Shapiro *et al.*, DL model. \bullet : this work, DL model. \triangle : this work, DHO model.

meaningful temperature dependence. The mean value of the gap energy is about 0.002 THz (8 μeV) with a possible enhancement of 0.001 or 0.002 THz at low temperature. It is seen that D obtained from using F_{DHO} is essentially independent of temperature for $T < 100$ K, whereas the use of F_{DL} shows a substantial decrease of D for $T < 100$ K. For $T > 50$ K the present results and those of Shapiro *et al.* are in agreement but for $T < 50$ K the present experiment shows less of a softening.

In Figs. 5 and 6 are reported the temperature evolution of the parameters measured at a single $Q = 0.040 \text{ \AA}^{-1}$. For $T \geq 13$ K the parameters are extracted from the above-mentioned analysis. Results at $T = 5$ and 10 K come from the second set of measurements and the intensities have been scaled to the first ones by common measurements at $T = 20$ K. Figure 4 shows that spin-wave energy using a DL analysis extrapolates to a finite energy at $T = 0$, although we point out again that no well-defined peak is present in the observed spectra at low temperatures. In Fig. 6 it is seen that the damping increases with decreasing temperature for both choices of $F(Q, \omega)$. The central peak intensity B_c increases sharply below $T = 20$ K. The spin-wave intensity B_s shows a gradual increase with decreasing temperature which cannot be understood within the framework of existing conventional spin-wave theories.

It is worthwhile to note that, despite the difficulty of the measurements, analyses using DL or DHO model yield a set of parameters which vary continuously with those obtained at higher temperatures. This emphasizes the fact that even in the absence of the low-energy part of the inelastic signal, which is masked by the huge elastic component, the information provided by the wings is quite meaningful, as long as the background remains low compared to the signal. Of course, the results of such an analysis can only be considered as possible hint of the low

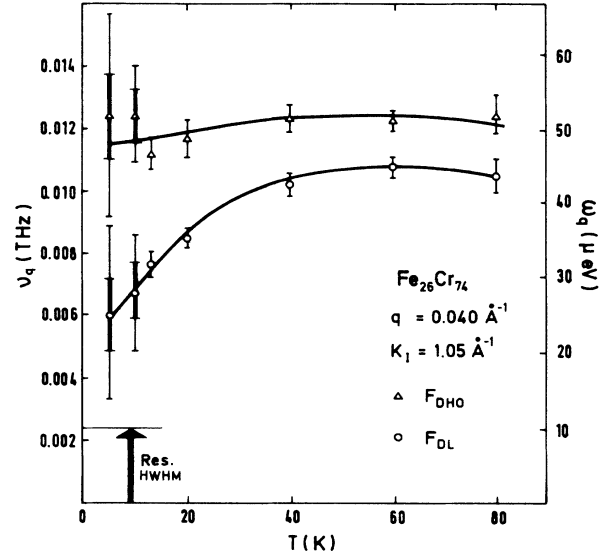


FIG. 5. The temperature dependence of spin-wave energy measured at $q = 0.04 \text{ \AA}^{-1}$ using F_{DHO} (\triangle) and F_{DL} (\circ). The error bars take into account the correlations between the adjusted parameters. For $T = 5$ or 10 K the thick part of the error bars correspond to neglecting the correlations.

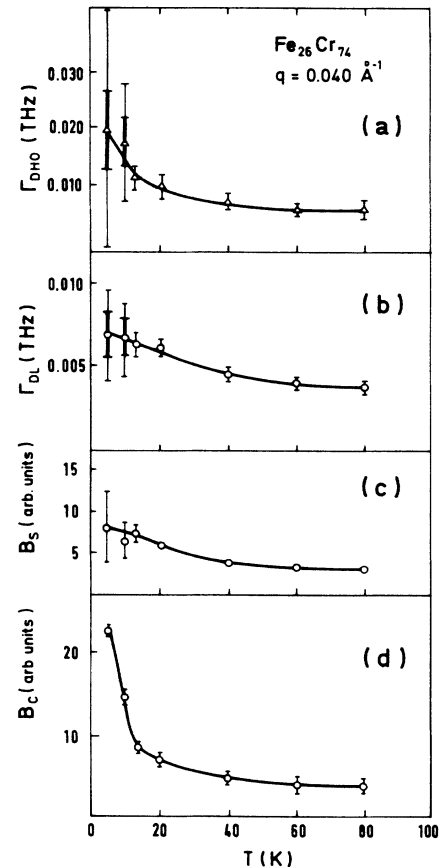


FIG. 6. Temperature dependence of parameters deduced from measurements at a single $q = 0.04 \text{ \AA}^{-1}$: (a) F_{DHO} , (b) Γ_{DL} , (c) B_s , the spin-wave intensity, (d) B_c , the central peak intensity. In (b) and (c) the values obtained from F_{DL} or F_{DHO} are nearly identical and only those obtained using F_{DL} are shown.

temperature behavior and definitely not as a proof of the existence of propagating spin waves on this temperature range.

IV. DISCUSSION

We presented new high-resolution measurements on $\text{Fe}_{26}\text{Cr}_{74}$ and showed that the spin waves are effectively present down to 13 K. The discrepancy with previous results of Shapiro *et al.*¹ is explained by the differences of experimental conditions. At low temperatures Shapiro *et al.* could not resolve their spectra into an elastic and an inelastic peak, because of their poor resolution. As the elastic part grows with decreasing temperatures their analysis yielded a quasielastic line whose linewidth was decreasing with T .

This emphasizes the crucial weight of the experimental conditions in neutron studies on this kind of systems. Using better resolution we have extended the temperature range where spin waves are clearly present, but again below about 10 K we are confronted with the experimental limits and we cannot get unambiguous results.

Various pictures have been proposed to describe the RSG, but none of them gives a specific quantitative prediction of the temperature dependence of the spin dynamics. Mean-field theories like that of Gabay and Toulouse¹⁰ preserve the ferromagnetic long-range order at any temperature, which implies the persistence of spin waves at low q values. In the random-field pictures,² the long-range order is destroyed at low temperature and the ferromagnetic spin-wave-like excitations could only exist for q values corresponding to wavelengths within the cluster's size. In the temperature range where spin waves are clearly observed, the q dependence of their dispersion and of the static transverse susceptibility can always be accounted for by conventional ferromagnetic laws assuming an appropriate damping. As far as the damping is decreasing with q faster than the spin-wave energy, we may infer long-range ferromagnetic order. But unfortunately, in this experiment, as in many similar neutron inelastic scattering measurements, we encounter the experimental limits, especially the impossibility of extending the measurements at lower q values, before arriving at definite conclusions. Hence, we may only make a speculative use of the data. Indeed the set of parameters which can be extracted from the data analysis are very different according to the model used to describe the spectral weight function. In the absence of ascertained mechanism to explain the spin-wave damping there is no way to choose between DL and DHO models. Both of them might as well be wrong and the elastic and inelastic components of the signal could be not independent as assumed up to now.

We are thus in the tantalizing situation where the experiments cannot by themselves decide of the physics of studied materials. The use of a phenomenological description for the spectral weight function gives rise to completely different physical pictures of the problem.

The decrease of D as given by the DL model could be interpreted as a softening of the system with eventually a complete collapse at very low temperature, indicating the disappearance of long-range ferromagnetic order. The DHO model favors the persistence of ferromagnetic heavily-damped spin-wave excitations at any temperatures.

The dynamics of RSG have now been carefully studied in several systems: $\text{Fe}_x\text{Cr}_{1-x}$,¹ $a\text{-Fe}_x\text{Mn}_{1-x}$,^{2,5} $\text{Ni}_{1-x}\text{Mn}_x$,⁴ $\text{Au}_{1-x}\text{Fe}_x$,³ $a\text{-Fe}_{1-x}\text{Ni}_x$,⁴ $a\text{-Fe}_{1-x}\text{Cr}_x$,^{7,8} $\text{Fe}_x\text{Al}_{1-x}$.⁹ All these systems present remarkable dynamic anomalies but, though many of the bulk properties such as the a - c susceptibility exhibit nearly universal behavior, it is not at all obvious that their dynamics present the same kind of universality. The studies on $\text{Ni}_{1-x}\text{Mn}_x$ (Ref. 4) and $a\text{-Fe}_{1-x}\text{Mn}_x$ (Ref. 5) show that after the abnormal decrease of the stiffness constant, it increases again when the temperature is further decreased. This behavior is not observed in the present experiment. But this could be due to the concentration dependence of the minimum of D which was shown to depend strongly on the composition in $a\text{-FeMn}$.¹¹ In $\text{Fe}_{26}\text{Cr}_{74}$ we are still rather near the ferromagnetic phase and the mechanism responsible for the stiffness recovering could take place at temperature beyond the limit of the study. On the other hand, measurements on $\text{Fe}_{1-x}\text{Al}_x$,⁹ with resolution comparable to that reported here, indicate that no propagating excitations are observed for $T \lesssim 150$ K, the inelastic part of the spectra being always quasielastic.

So we are led to the conclusion that the dynamical behavior of RSG is at least more intricate than was thought after the first studies. It might even be possible that there is no universal dynamical behavior for these systems. It is not obvious to find a physical parameter which could be a clue to explain the differences between the studied systems. The origin of the anomalies is certainly related to the frustration resulting from competing interactions and indeed the stiffness constant is related to these interactions. The composition of the different systems leads to different kinds of interactions involved in the magnetic properties. Let us also note that all these systems are metallic and the metallic character itself could play a key role in their behavior, as it likely facilitates an averaging of the electronic properties of the systems.

We have shown the importance of high-resolution and low-temperature studies on RSG in order to characterize their dynamics. It is important that other RSG systems be studied in the same manner in order to gain a better understanding of the low-temperature phase. In addition theoretical studies are also lacking: models providing a specific spectral weight function would allow a more pertinent analysis of the experimental data.

ACKNOWLEDGMENT

The laboratoire Léon Brillouin is a Laboratoire commun Commissariat à l'Énergie Atomique, Centre National de la Recherche Scientifique.

- *Permanent address: Brookhaven National Laboratory, Upton, NY 11973.
- ¹S. M. Shapiro, C. R. Fincher, A. C. Palumbo, and R. D. Parks, *Phys. Rev. B* **24**, 6661 (1981).
- ²G. Aeppli, S. M. Shapiro, R. J. Birgeneau, and H. S. Chen, *Phys. Rev. B* **29**, 2589 (1984).
- ³A. P. Murani, *Phys. Rev. B* **28**, 432 (1983).
- ⁴B. Hennion, M. Hennion, F. Hippert, and A. P. Murani, *J. Phys. F* **14**, 489 (1984).
- ⁵B. Hennion, M. Hennion, I. Mirebeau, and F. Hippert, *Physica* **136B**, 49 (1986).
- ⁶R. W. Erwin, J. W. Lynn, J. J. Rhyne, and H. S. Chen, *J. Appl. Phys.* **57**, 3473 (1985).
- ⁷J. P. Wicksted, S. M. Shapiro, and H. S. Chen, *J. Appl. Phys.* **55**, 1697 (1984).
- ⁸P. Mangin, D. Boumazouma, C. Tête, R. W. Erwin, and J. J. Rhyne, *J. Appl. Phys.* **61**, 3619 (1987).
- ⁹K. Motoya, S. M. Shapiro, and Y. Muraoka, *Phys. Rev. B* **28**, 6183 (1983).
- ¹⁰M. Gabay and G. Toulouse, *Phys. Rev. Lett.* **47**, 201 (1981).
- ¹¹S. Lequien and B. Hennion (unpublished); S. Lequien, thesis, Orsay, 1988.